PASJ: Publ. Astron. Soc. Japan **59**, 1107–1113, 2007 December 25

Astrometry of H_2O Masers in Nearby Star-Forming Regions with VERA I. IRAS 16293−2422 in ρ Oph East

Hiroshi IMAI,[1,2] Kohichiro NAKASHIMA,[2] Takeshi BUSHIMATA,[3,4] Yoon Kyung CHOI,[3,5] Tomoya HIROTA,[3] Mareki HONMA,[3,6] Koji HORIAI,[7] Noritomo INOMATA,[2] Kenzaburo IWADATE,[3,7] Takaaki JIKE,[3,7] Osamu KAMEYA,[3,6,7] Ryuichi KAMOHARA,[3] Yukitoshi KAN-YA,[3,8] Noriyuki KAWAGUCHI,[3,6,7] Masachika KIJIMA,[3,6] Hideyuki KOBAYASHI,[3,6,7] Seisuke KUJI,[3,7] Tomoharu KURAYAMA,[3,7] Seiji MANABE,[3,6,7] Takeshi MIYAJI,[3,7] Takumi NAGAYAMA,[2] Akiharu NAKAGAWA,[1] Chung Sik OH,[3,5] Toshihiro OMODAKA,[1,2] Tomoaki OYAMA,[3,7] Satoshi SAKAI,[3,7] Seiichiro SAKAKIBARA,[2] Katsuhisa SATO,[3,7] Tetsuo SASAO,[9,10] Katsunori M. SHIBATA,[3,6,7] Rie SHIMIZU,[2] Motonobu SHINTANI,[2] Yoshiaki SOFUE,[1,2] Kasumi SORA,[2] Hiroshi SUDA,[3,7] Yoshiaki TAMURA,[3,6,7] Miyuki TSUSHIMA,[2] Yuji UENO,[7] and Kazuyoshi YAMASHITA[3,6]

[1]*Department of Physics, Faculty of Science, Kagoshima University, 1-21-35 Korimoto, Kagoshima 890-0065*
[2]*Graduate School of Science and Engineering, Kagoshima University, 1-21-35 Korimoto, Kagoshima 890-0065*
[3]*Mizusawa VERA Observatory Mitaka Office, National Astronomical Observatory, 2-21-1 Osawa, Mitaka, Tokyo 181-8588*
[4]*Space VLBI Project, National Astronomical Observatory, 2-21-1 Osawa, Mitaka, Tokyo 181-8588*
[5]*Department of Astronomy, The University of Tokyo, Bunkyo-ku, Tokyo 113-8654*
[6]*Graduate University for Advanced Studies, 2-21-1 Osawa, Mitaka, Tokyo 181-8588*
[7]*Mizusawa VERA Observatory, National Astronomical Observatory, 2-12 Hoshigaoka, Mizusawa-Ku,Oshu-shi, Iwate 023-0861*
[8]*Department of Astronomy, Yonsei University, 134 Shinchong-dong, Seodaemun-gu, Seoul 120-749, Republic of Korea*
[9]*Department of Space and Information Technology, Ajou University, Suwon 443-749, Republic of Korea*
[10]*Korean VLBI Network, Korea Astronomy and Space Science Institute, P.O. Box 88, Yonsei University, 134 Shinchon-dong, Seodaemun-gu, Seoul 120-749, Republic of Korea*
(HI) hiroimai@sci.kagoshima-u.ac.jp

(Received 2007 June 4; accepted 2007 July 15)

Abstract

We report on results of multi-epoch VLBI observations of H_2O masers associated with a low-mass young stellar object, IRAS 16293−2422 in ρ Oph East, and a fringe-phase and position reference source, ICRF J162546.8−252738, using the VLBI Exploration of Radio Astrometry (VERA) for high-precision astrometry. We obtained an annual parallax of a maser feature to be $\pi = 5.6^{+1.5}_{-0.5}$ mas, corresponding to a distance of $D = 178^{+18}_{-37}$ pc. We also found 10 relative proper motions of maser features with respect to the maser feature mentioned above. The motion of the accompanying young stellar object (YSO) has already been found in thermal continuum emission previously observed with the Very Large Array. The intrinsic motions of masers have been estimated from the relative proper motions after the YSO's motion is subtracted from, and a systemic secular motion of the position reference feature is added to the proper motions originally measured. The intrinsic maser kinematical structure may trace a bipolar outflow.

Key words: astrometry — masers — stars: formation — stars: individual (IRAS 16293−2422) — ISM: jets and outflows

1. Introduction

High-precision astrometry for H_2O maser sources using high angular resolution achieved by very long baseline interferometry (VLBI) provides a great opportunity to directly measure distances to young stellar objects (YSOs) and evolved stars distributed in the whole Galaxy (e.g., Kurayama et al. 2005; Hachisuka et al. 2006; Honma et al. 2007; Hirota et al. 2007, 2008; Imai et al. 2007). Also, H_2O maser astrometry should provide a great impact on studies of individual H_2O maser sources. Because each H_2O maser source consists of many compact maser features with a typical size of 1 AU (e.g., Elitzur 1992), their proper motions are measurable within 1–2 yr or shorter. Thus, we can elucidate the three-dimensional velocity fields of molecular gas regions in the very vicinity of YSOs, Mira variables, and central stars of pre-planetary and planetary nebulae. However, any previous proper motion measurement requested a position reference maser feature, with respect to which proper motions of other maser features were *relatively* measured. In such a case, information on the proper motion of the position reference feature itself is missing, which leads to ambiguity in interpretation of the revealed maser kinematics. For instance, it is difficult, in principle, to distinguish between bipolar and monopolar outflows from two groups of maser features moving in opposite directions. A similar ambiguity occurs when distinguishing between an outflow and a rotating disk. Suppose that proper motions of maser features are measured with respect to an extragalactic quasar as position references, so that maser positions are determined in a common coordinate system at every observation epoch. We can then find the intrinsic motions of maser features after subtracting an annual parallax and

Table 1. Parameters of VERA observations and data reduction for IRAS 16293−2422 and ICRF J162546.8−252738.

Epoch	Code*	Date (yy/mm/dd)	VERA† telescopes	Rec.‡	Δv§	Beam‖ (mas)	Noise(1-σ) (Jy b^{-1})	N_f#	Remark**
1	r03283a	03/10/10	MZ, IR, IS	1 K	0.21	10.0×0.7 −32°	0.9	3	
2	r03301a	03/10/28	MZ, IR, OG, IS	2 K	0.42	5.6×1.0 −31°	1.2	3	A, P
3	r04034b	04/02/03	MZ, IR, OG, IS	2 K	0.21	2.0×1.0 −17°	0.5	7	A, P
4	r04056b	04/02/25	MZ, IR, OG, IS	2 K	0.21	3.5×0.8 −28°	15.4	4	P
5	r04079a	04/03/19	MZ, IR, OG, IS	2 K	0.21	2.6×0.8 −31°	0.4	7	A, P
6	r04117b	04/04/26	MZ, OG, IS	2 K	0.21	2.0×0.6 −18°	1.5	6	P
7	r04147b	04/05/26	MZ, IR, OG, IS	1 K	0.21	1.9×1.0 −18°	0.8	4	P
8	r04204a	04/07/22	MZ, IR, OG, IS	1 K	0.21	2.2×0.8 −25°	0.1	4	P
9	r04270a	04/09/26	MZ, IR, OG, IS	1 K	0.21	2.0×1.2 −25°	0.2	2	P
10 ...	r04299a	04/10/25	MZ, IR, OG	1 K	0.21	2.4×1.1 −13°	0.3	2	P
11 ...	r04324a	04/11/19	MZ, IR, OG, IS	1 K	0.21	2.4×1.1 −13°	0.1	2	P
12 ...	r05292a	05/10/19	MZ, IR, OG, IS	2 K	0.42	2.5×0.8 −30°	0.4	2	A, P
13 ...	r05322a	05/11/18	MZ, IR, OG	2 K	0.42	2.6×1.0 −30°	0.5	1	A, P
14 ...	r05354c	05/12/20	MZ, OG, IS	2 K	0.42	2.4×0.6 −25°	0.2	1	P
15 ...	r06017a	06/01/17	MZ, IR, OG, IS	2 K	0.42	2.2×0.8 −34°	0.2	1	A, P
16 ...	r06053b	06/02/22	MZ, IR, OG, IS	2 K	0.42	2.1×1.1 −30°	0.2	1	P

* Code name of the observation, which has a form such as rYYDDDx, where YY denotes the last two-digit number of the observation year, DDD the day of the year of the observation epoch, $x = a, b$, ... alphabetical code of the observations made in the same date.
† Participating telescopes in VERA. MZ: at Mizusawa, Iwate, IR: at Iriki, Kagoshima, OG: at Ogasawara Islands, Tokyo, and IS: at Ishigakijima, Okinawa.
‡ Used recorder, 1 K: SONY DIR1000, 2 K: SONY DIR2000.
§ Spectral channel spacing in km s^{-1} .
‖ Synthesized beam made with naturally weighted visibilities; major and minor axis lengths and position angle.
Number of detected maser features.
** A: Correction for atmospheric zenith delays is valid. P: Phase-reference maser map is valid for astrometry.

a secular motion of the accompanying stellar object (for the latter if measurable in other observations) from the maser motions originally measured.

We have applied H_2O maser astrometry to study star formation. In the present paper, we report on astrometric results for H_2O masers associated with the low-mass YSO, IRAS 16293−2422 (hereafter abbreviated as I16293) observed with the VLBI Exploration of Radio Astrometry (VERA),[1] which is dedicated for high-precision maser astrometry (e.g., Honma et al. 2000). Previous VLBI observations found a group of H_2O maser features whose spatio-kinematical structure is well modeled by an infalling-rotating gas disk as well as a few features that may be associated with an outflow with an axis roughly perpendicular to the disk (Imai et al. 1999, hereafter IIM99). The existence of such a disk has been supported on the larger scale (> 100 AU, e.g., Remijan & Hollis 2006; Takakuwa et al. 2007). However, IIM99 did not perform any measurement of maser proper motions. On the basis of a relative proper motion of a maser feature, Wootten et al. (1999) claimed that the masers should be associated with an outflow. Note that because these previous VLBI observations lose the absolute coordinates of maser features, it was difficult to unambiguously obtain a dynamical interpretation for the maser spatio-kinematics.

The distance to I16293 has been estimated to be 160 pc based on the optical and infrared photometry of stars associated with the ρ Oph cloud (Chini 1981). More recently, a distance of 120 pc was obtained while taking into account reddening in the optical Hipparcos and Tycho catalog data (Knude & Høg 1998), but the high extinction toward the cloud limits the optical reddening techniques to the outer edges of the cloud.

In the present paper, we directly estimate the intrinsic motions of H_2O masers in I16293 and the distance to I16293 in the annual-parallax technique. Section 2 describes the VERA observations and data analysis in detail. Section 3 presents the revealed maser spatio-kinematical structure and astrometric results. Section 4 discusses the distance measurement and the intrinsic motions of H_2O masers.

2. Observations and Data Reduction

VERA observations of the I16293 H_2O masers were made from 2003 October to 2004 November (epochs 1–11) and from 2005 October to 2006 February (epochs 12–16). Table 1 gives a summary of these observations and maser images. At each epoch, the observation was made for 4–6 hr, including scans of I16293 and the fringe phase and position reference source, ICRF J162546.8−252738 (hereafter abbreviated as J1625), using VERA's dual-beam system. These two sources are separated by 1.°79. The signals were digitized in four quantization levels in the ADS1000 unit, and then divided into 16 base band channels (BBCs) in the digital filter unit, each of which had a bandwidth of 16 MHz (Iguchi et al. 2005). The

[1] VERA observatory is a branch of the National Astronomical Observatory, an interuniversity research institute operated by the Ministry of Education, Culture, Sports, Science and Technology.

Table 2. Relative proper motions of H_2O masers in IRAS 16293−2422.

Maser feature* (IRAS 16293−2422: I2007)	Offset (mas)		Proper motion (mas yr^{-1})				Radial motion V_{LSR} (km s^{-1})		Detection at 11 epochs†										
	RA	Dec	μ_x	$\sigma\mu_x$	μ_y	$\sigma\mu_y$	V_z	ΔV_z	1	2	3	4	5	6	7	8	9	10	11
1	602.64	330.04	19.91	2.25	16.28	2.34	0.65	1.26	○	○	×	×	×	×	×	×	×	×	×
2‡	616.63	321.20	28.02	1.77	51.62	3.39	2.02	0.73	×	×	×	×	×	○	○	○	×	×	×
3§	637.41	341.92	46.79	1.60	25.45	2.50	2.79	1.05	×	×	×	×	×	×	×	×	○	○	×
4	−80.70	36.72	1.98	0.35	−1.09	0.50	4.19	0.49	×	×	○	○	○	○	×	×	×	×	×
5‖	0.00	0.00	0.00	0.04	0.00	0.08	4.43	0.95	○	○	○	○	○	○	○	○	○	○	○
6	−1.34	2.91	−4.43	1.90	10.98	3.75	4.61	0.39	×	×	○	○	×	×	×	×	×	×	×
7	−5.91	2.11	−4.26	0.51	1.26	0.79	4.64	0.49	×	×	×	×	○	○	×	○	×	×	×
8	0.63	−0.62	2.58	0.37	2.06	0.33	5.07	0.53	×	×	×	×	○	○	×	○	×	×	×
9	−1.56	0.04	−7.71	1.26	10.75	2.11	5.07	0.47	×	×	×	×	○	○	×	×	×	×	×
10	−0.31	0.16	1.71	0.71	−2.29	0.29	5.07	0.37	×	×	×	×	○	×	○	×	×	×	×

* Water maser features detected toward IRAS 16293−2422. The feature is designated as IRAS 16293−2422: I2007 *N*, where *N* is the ordinal source number given in this column (I2007 stands for sources found by Imai et al. and listed in 2007).
† ○: detection, ×: negative detection.
‡ Feature *c*.
§ Feature *b*.
‖ Feature *a*, the position reference feature.

BBC outputs were recorded with either a SONY DIR1000 or DIR2000 recorder; they recorded the data in only 2 and all of the 16 BBCs, respectively. One of the BBCs was assigned to the frequency of H_2O maser emission in I16293.

A data correlation was made with the Mitaka FX correlator. The accumulation period of the correlation was set to 1 s. The correlation outputs consisted of 512–1024 and 32–64 spectral channels for the H_2O maser and reference continuum emission, respectively. A velocity spacing of 0.21 km s^{-1} or 0.42 km s^{-1} was obtained in each spectral channel for the H_2O maser emission.

Data reduction was mainly made with the NRAO AIPS package. To obtain maser image cubes and final maser maps, we adopted the normal procedure, in which fringe-fitting and self-calibration were performed using the data in the Doppler-velocity channel with the brightest H_2O maser spot (velocity channel component) at $V_{LSR} = 4.4$ km s^{-1} as a reference. There, all maser spot positions were measured with respect to that of the reference spot. Column 7 in table 1 gives parameters of the synthesized beam at each epoch. The identification of an H_2O maser feature (a cluster of maser spots or velocity components tracing a physical gas clump) was made using the same procedure shown in several previous papers (e.g., Imai et al. 2000), in which the feature position is defined as a brightness peak in the feature.

For astrometry, we need special processes, described as follows. At first, delay-tracking is again performed for the correlated data using better delay-tracking models calculated with the original software equivalent to the GFSC CALC9 package. The delay-tracking solutions included delay contributions from the atmosphere, which were estimated using the global positioning system (GPS) data. The details are described in Honma et al. (2007). At second, delay differences between the two source directions, due to unknown residuals in zenith atmospheric delays, were estimated with the AIPS task DELZN using data of the phase-reference continuum source. This correction is valid only for data replayed from the DIR2000 recorder, which had an effective bandwidth of 240 MHz in group-delay measurements using the continuum data in the present observations. Column 10 in table 1 indicates the epochs when this correction was valid or invalid. At third, fringe-fitting and self-calibration were then performed using the continuum data, whose solutions were applied to the data of maser emission. Finally, differences in instrumental delays between two signal paths in the dual beam system were calibrated using the differential delays, which were measured using artificial noise signals injected at the same time into the two receivers. The efficiency of fringe-phase compensation or coherence integration was relatively poor for the I16293–J1625 pair, because the separation of the sources is not ideally short. In addition, VERA's (u, v) plane coverage for I16293 was limited at a low declination ($\delta = -24°$) and reduced by weather, operational, and data-calibration problems. At several epochs, the maser images obtained in the phase-referencing technique were significantly defocused. To obtain each of final CLEANed maser images, we found the highest feature peak intensity achieved by the best allocation of CLEAN boxes in the deconvolution image.

3. Results

3.1. Spot Sizes and Position Uncertainties of Maser Features

The I16293 H_2O maser emission flared up over 48000 Jy in flux density in 2003 September. The observed properties, especially the elongated geometry of the flared maser feature, IRAS 16293−2422: I2007 *5* = Feature *a* (shown later), was similar to that found in the flared H_2O maser feature in Orion KL (Matveyenko et al. 2004; Shimoikura et al. 2005). Because I16293 is very close to the Sun, apparent sizes of maser spots should be so large that they are significantly spatially

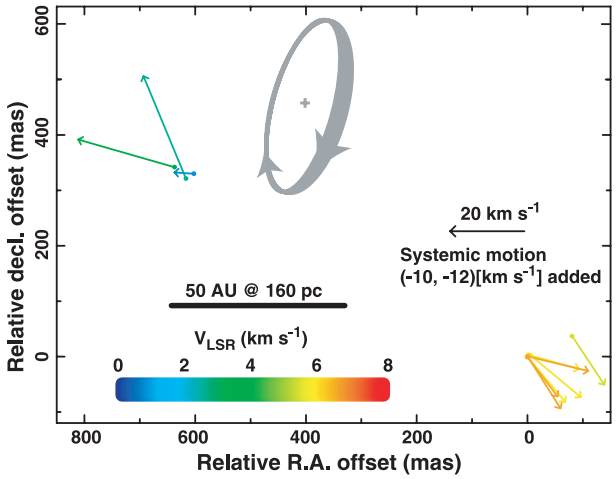

Fig. 1. Relative proper motions of H_2O maser features in IRAS 16293−2422 detected at the first 11 epochs. The root of an arrow indicates the location of the feature at the first of the epochs when the maser feature was detected. The length and the direction of an arrow indicate the speed and direction of the maser proper motion, respectively. The coordinate origin is located at the position of Feature *a* at epoch 1. The proper-motion vector is shown with a systemic motion vector of Feature *a* added (see main text). The grey plus and the surrounding elliptical ring indicate the location of a YSO and the inclination and rotation direction of the surrounding gas disk, respectively, which are proposed by IIM99.

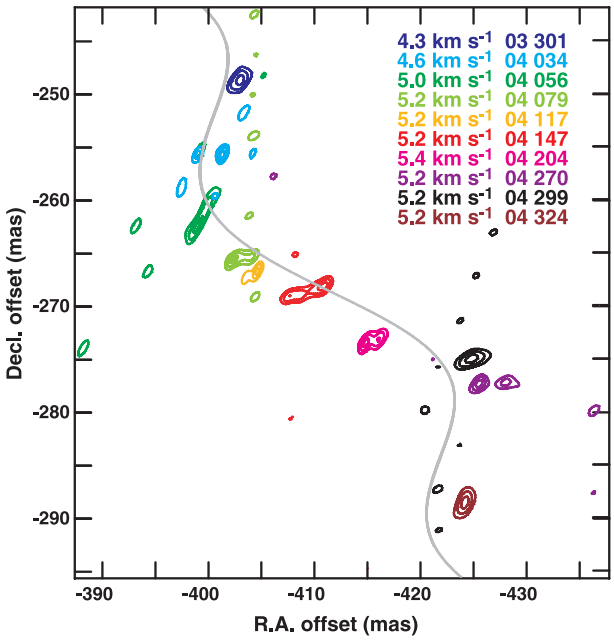

Fig. 2. Temporal variation of the brightness distribution of Feature *a*. The feature position has been measured with respect to the delay-tracking center in data correlation located at RA(J2000) = $16^h32^m22^s.85$, Dec(J2000) = $-24°28'36''.4$. A grey curve indicates the maser feature motion with an annual parallax of 5.6 mas and a systemic motion of $(-20.6 \pm 0.7, -32.4 \pm 2.0)$ [mas yr^{-1}].

resolved with the synthesized beam. In fact, the maximum correlated flux density of the flared feature was only ~ 3400 Jy. This affected the accuracy of the maser position estimation. Statistical errors of the relative positions of maser spots, which were estimated from the signal-to-noise ratios, ranging over 0.01–0.09 mas. The uncertainty of the relative positions of the maser feature, however, may be worse by one order of magnitude than the statistical errors of the maser spot positions, or comparable to the synthesized beam size given in table 1.

3.2. *Relative Proper Motions of Maser Features*

Table 2 gives the positions and *relative* proper motions of maser features with respect to the position reference feature, IRAS 16293−2422: I2007 *5* (designated as Feature *a*). We detected 10 proper motions, in each of which the same maser feature was identified at least at two of the successive observation epochs. During the years 2005 and 2006, only one faint (≤ 2 Jy) maser feature at $V_{LSR} = 6.0$ km s^{-1} was identified, but it is not reported here.

Figure 1 shows the positions and the proper motions of the maser features. A systemic motion, $(\Delta\mu_X, \Delta\mu_Y) = (-13.1, -16.3)$ [mas yr^{-1}], corresponding to a velocity vector of $(\Delta V_X, \Delta V_Y) = (-10, -12)$ [km s^{-1}], is added to all of the feature motions. The systemic motion corresponds to an intrinsic motion of Feature *a* with respect to the accompanying YSO, IRAS 16293−2422 A2, detected in centimeter and millimeter continuum emission (Chandler et al. 2005). The three-dimensional velocity field of the maser features suggests the existence of a bipolar outflow in the direction of $PA \sim 60°$ east from north without any possibility of a monopolar outflow. The systemic motion adopted here and the maser velocity field are discussed in more detail in subsection 4.2.

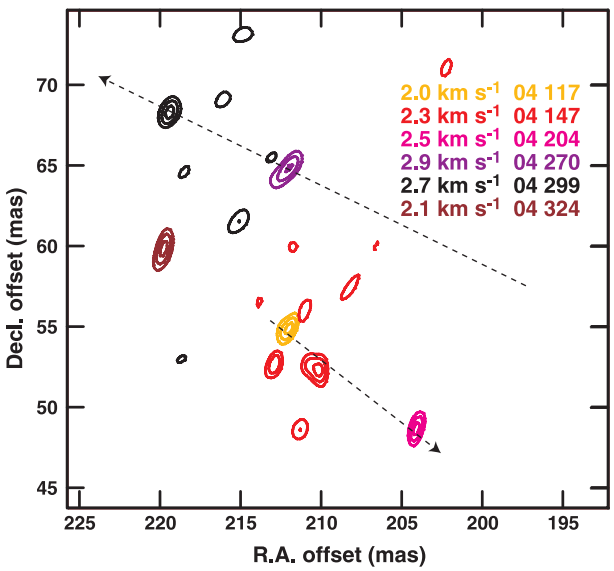

Fig. 3. Same as figure 2, but Features *b* and *c* (upper and lower features, respectively). The dashed arrow indicates the vector of the feature proper motion for 100 d.

3.3. *Maser Astrometry and Annual-Parallax Distance*

Out of 10 maser features with measured *relative* proper motions, we consider the motions of Feature *a* and the maser features IRAS 16293−2422: I2007 *3* and *2* (designated as Features *b, c*, respectively) with respect to the position reference, J1625. Figures 2 and 3 show temporal position

variations of the three features during epochs 2–11. Although Feature *a* has a temporal variation in the brightness distribution, the feature motion exhibits an annual parallax and a systemic (constant velocity) motion. Figure 4 shows the best-fit maser motion model for Feature *a*.

We obtained an annual parallax of Feature *a* to be 5.6 ± 0.5 mas. The uncertainty contains statistical and systematic errors (0.4 mas and 0.1 mas, respectively), and gives a lower limit of 5.1 mas to the estimated parallax. Assuming that a position error of the maser feature is equal to the half width of the synthesized beam shown in table 1, we estimated the statistical error of the parallax to be 0.4 mas. Because, as shown in figure 2, odd positions of the features are found, an estimation of the annual parallax was made not only using all 10 epoch positions, but also using 9 epoch positions, excluding one of the odd positions (at epochs 9, 10). The parallaxes estimated using different combinations of epoch positions are converged within 0.1 mas, which corresponds to one of the factors of the systematic error. When adopting only statistical feature position errors (0.1–0.3 mas), a parallax of 7.1 mas was obtained, which gave an upper limit to the estimated parallax. In the case of equal position errors at all epochs, a parallax of 5.7 mas was obtained. Finally, we obtained the annual parallax to be $\pi = 5.6^{+1.5}_{-0.5}$ mas, which corresponds to a distance to I16293 of $D = 178^{+18}_{-37}$ pc. The estimated uncertainty of parallax is reasonable when taking into account the standard deviations of the maser positions of 1.9 mas and 2.9 mas in the R.A. and Decl. directions, respectively, from the model fit curve. The estimated distance is consistent with that previously adopted (160 pc: Chini 1981) within this uncertainty.

Here, the maser feature locations are compared with the locations of YSOs in I16293 in the common coordinate system. Figure 5 shows the locations of two maser features on continuum (3.7 cm and 1 mm) emission images obtained by Chandler et al. (2005). The H_2O maser and continuum source observations were made in the same season within 2 months, during which the maser and continuum sources moved within 15 mas (see also figures 2 and 3). The two maser features, one is Feature *a* and another close to Features *b* and *c*, seem to be associated with the continuum source IRAS 16293−2422 Aa, which is located between the two features. The proper motion of Feature *a* $(\mu_X, \mu_Y) = (-20.6 \pm 0.7, -32.4 \pm 2.0)$ [mas yr^{-1}] is faster than those of the continuum sources A1 and A2 $(\mu_X, \mu_Y) = (-1.9, -27.8)$ and $(-7.5, -16.1)$ [mas yr^{-1}], respectively. The difference of the maser and continuum source proper motion vectors may correspond to the intrinsic motion vector of Feature *a* in the YSO system, which is added to the relative proper motion vectors of masers in order to represent the intrinsic maser proper motions. The intrinsic motion of Feature *a* is roughly parallel to the direction of the bipolar outflow seen in the maser velocity field (figure 1).

4. Discussion

4.1. *Feasibility of an Annual Parallax Measurement with H_2O Maser Emission*

VERA has already achieved an astrometric accuracy of ~ 50 μas in nearly ideal cases, in which a maser–quasar pair is located at a high declination ($\delta \geq 20°$); both of the pair sources have compact and simple brightness structures, and are bright enough for fringe-phase compensation, and its angular separation is shorter than 1° (e.g., Honma et al. 2007). The case in the I16293 H_2O masers is a completely opposite case from the ideal one. The most severe factor of

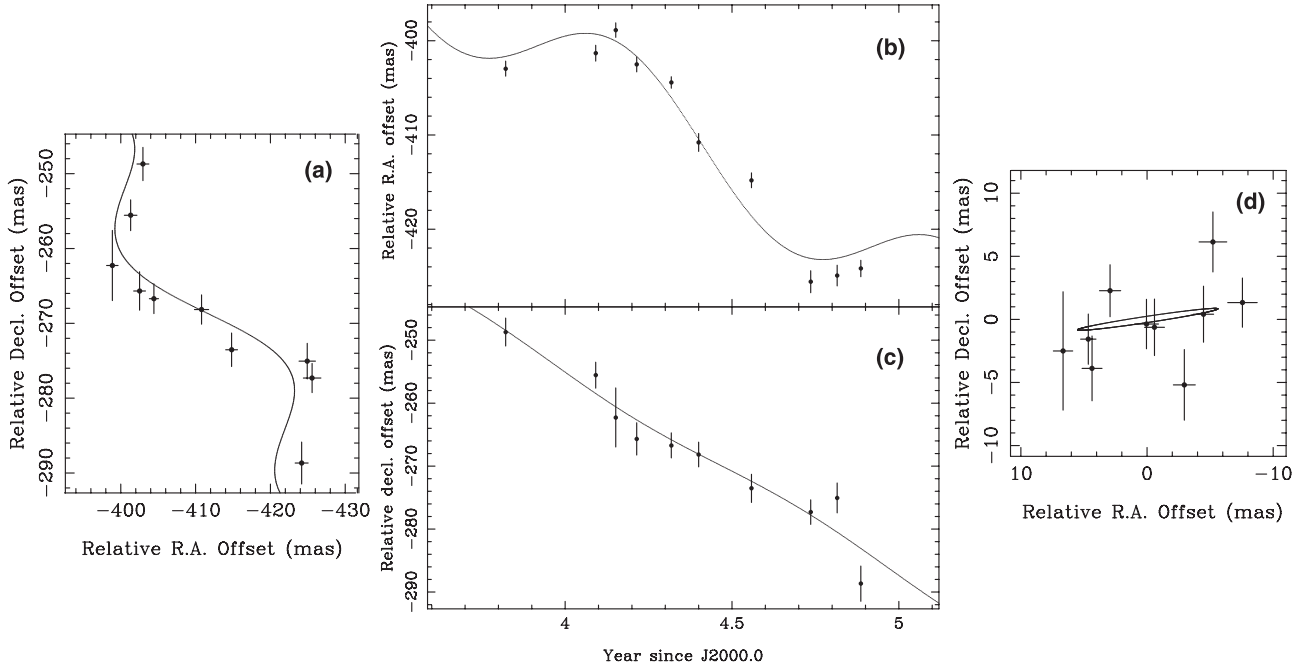

Fig. 4. Position of the maser feature *a* at all observation epochs and the best-fit maser motion model (a solid curve). The solid curve indicates the feature motion with the best-fit parameters; an annual parallax of 5.6 mas and a systemic motion of $(-20.6 \pm 0.7, -32.4 \pm 2.0)$ [mas yr^{-1}]. (a) RA and Dec offsets on the sky. (b) and (c) RA and Dec offsets against time. (d) Relative offsets with a position offset and the secular proper motion subtracted.

the poor astrometric accuracy in IRAS 16293−2422 may be a temporal variation in the brightness structure of a maser feature. In fact, an LSR velocity of Feature *a* at the flux peak varied by $\sim 1\,\mathrm{km\,s^{-1}}$, and another maser feature nearby Feature *a* has significantly affected the Gaussian brightness model fitting (see figure 2). This may lead to a position fluctuation over the synthesized beam size (1–2 mas). Also note that only one of 10 maser features detected their proper motions has survived for one year. Relatively short lifetimes of H_2O maser features have often been recognized in low-mass star-forming regions ($t \sim 1$–2 months, e.g., Claussen et al. 1996), which makes annual parallax measurements difficult. In such a situation, misidentification of the same maser features from one epoch to another occasionally occurs, which induces a larger uncertainty in the kinematical parameters of the maser feature motions. Nevertheless, H_2O maser astrometry is still a unique application for estimating the distances to star-forming molecular clouds, because the maser sources are unambiguously associated with the molecular clouds. They usually have few bright point sources that can be observed with high angular resolution for astrometry.

4.2. *Dynamical Relation of the Maser Features to the Continuum Sources in IRAS 16293−2422*

In I16293, fortunately, we can directly compare the locations and motions of the H_2O maser features with those of the YSOs, themselves, traced by continuum emission. The maser spatio-kinematics shown in figure 1 suggests the existence of a bipolar outflow. The major axis of the outflow is roughly consistent with that found in SiO emission (Hirano et al. 2001) and that of a high-velocity component in the HCN($J = 4$–3) emission (Takakuwa et al. 2007). The red-shifted maser component (close to Features *b* and *c*, a grey cross in figure 5) is located $\sim 0\farcs2$ south-east from the continuum source A2, roughly at the middle of sources A1 and A2. Sources A2 and A1 are expected to pinpoint a YSO and a shock region caused by outflow from the protostar, respectively. Thus, both of the blue-shifted and red-shifted components may be associated with shocks in the outflow, as suggested by Wootten et al. (1999). Note that the relative proper-motion vector of source A1 is perpendicular to the outflow direction, while the position of source A2 relative to source B has remained constant over the past 17 years. The origin of source A1 is still obscure (Chandler et al. 2005).

On the contrary, IIM99 has suggested the existence of an infalling-rotating gas disk in the H_2O maser region, but the present work does not rule out IIM99's suggestion. According to figure 5, the YSO driving the bipolar outflow should be located at around (400, 450)[mas] in figure 1. Note that the brightness peak of the 345 GHz continuum emission is also located at the same position (Takakuwa et al. 2007). The more blue-shifted maser features ($V_{\mathrm{LSR}} \leq 0\,\mathrm{km\,s^{-1}}$) had been detected not in the present paper, but in previous work (Wootten 1993; IIM99). They had been located closer to two continuum sources, corresponding to sources A1 and A2 (Mundy et al. 1992; Chandler et al. 2005) than to the blue-shifted maser features found in the present works. The more red-shifted maser features ($V_{\mathrm{LSR}} \geq 5\,\mathrm{km\,s^{-1}}$) were located at around (400, −50)[mas] in the same previous work. Thus, maser features possibly associated with the gas disk were located at the middle of the approaching and receding sides of the bipolar outflow found in the present paper. Note that the direction of elongation in the more red-shifted and more blue-shifted maser feature distribution, roughly the north–south direction, is consistent with that of the distribution of HCN emission (Takakuwa et al. 2007), which suggests the existence of a circum-protostellar disk traced by this emission. However, the maser association with such a gas disk should be confirmed by measuring the 3D motions of maser features. In Serpens SMM1, for example, the existence of a rotating accretion disk is suggested, where H_2O masers are associated with the interacting region of the bipolar jet with the disk and the maser kinematics is dominated by the jet (Moscadelli et al. 2006).

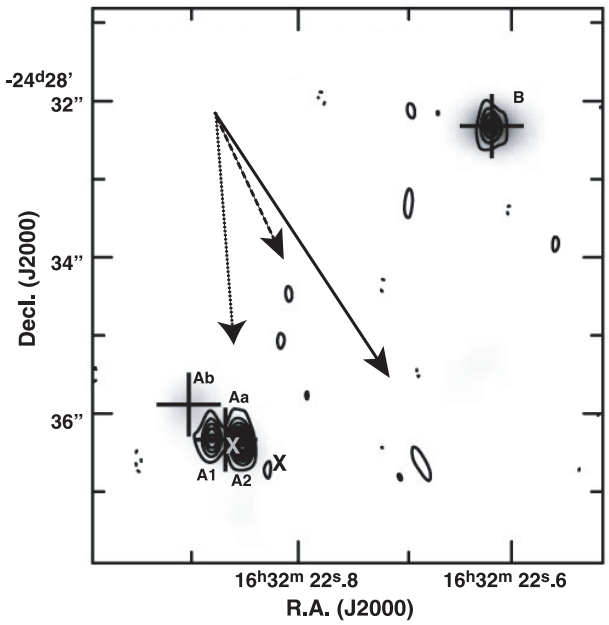

Fig. 5. Locations of two H_2O maser features detected on 2003 October 28 (cross) on the map of 3.7 cm (contour) and 1 mm (grey scale) continuum emission obtained on 2003 August 26 and 2004 July 27, respectively (Chandler et al. 2005). One maser feature (Feature *a*, black cross) was located at $V_{\mathrm{LSR}} = 0.9\,\mathrm{km\,s^{-1}}$, RA $= 16^{\mathrm{h}}32^{\mathrm{m}}22\farcs82048$, Dec $= -24°28'36\farcs6485$ in J2000, and another (close to Features *b* and *c*, grey cross) at $V_{\mathrm{LSR}} = 4.3\,\mathrm{km\,s^{-1}}$, RA $= 16^{\mathrm{h}}32^{\mathrm{m}}22\farcs86474$, Dec $= -24°28'36\farcs3172$. Big plus signs indicate the locations of the brightness peaks of 1 mm continuum emission (Aa, Ab, and B). The dotted, dashed, and solid arrows indicate the proper-motion vectors of the 3.7 cm continuum sources, A1 and A2 (left and right contour peaks near the source Aa, respectively, designated by plus symbols) $(\mu_{\mathrm{X}}, \mu_{\mathrm{Y}}) = (-1.9, -27.8)$, $(-7.5, -16.1)$ [mas yr^{-1}] (Chandler et al. 2005) and the maser feature, Feature *a* $(\mu_{\mathrm{X}}, \mu_{\mathrm{Y}}) = (-20.6 \pm 0.7,\ -32.4 \pm 2.0)$ [mas yr^{-1}], respectively (100 times of the annual motion).

5. Conclusions

In H_2O maser astrometry using VERA, we obtained the annual parallax of I16293 to be $\pi = 5.6^{+1.5}_{-0.5}$ mas, and inferred the distance to I16293 to be $D = 178^{+18}_{-37}$ pc. We also obtained the proper motions of three maser features with respect to the position reference source, J1625. By comparing the motion of the position reference feature, Feature *a* with that of the

accompanying YSO, we found the intrinsic internal motions of H_2O masers. They unambiguously suggest the existence of a bipolar outflow in the NEE–SWW direction, which may be located at the very vicinity of the root of a bipolar outflow found on a larger scale in SiO emission (Hirano et al. 2001). However, it does not rule out a possibility that an infalling-rotating gas disk exists, as suggested in the previous observations (IIM99), because the maser features found in the present paper may not trace the same maser region as that found in IIM99. Thus maser astrometry enables us to find the maser features associated with both a bipolar outflow and a circum-protostellar gas disk found in the present and previous observations, respectively.

We acknowledge all staff members and students who have helped in array operation and in data correlation of VERA. TH, HI, and HK have been supported by Grant-in-Aid for Scientific Research from the Japan Society for the Promotion Science (16540224). HI has also been financially supported by Grant-in-Aid for Young Scientists (B) from the Ministry of Education, Culture, Sports, Science and Technology (18740109).

References

Chandler, C. J., Brogan, C. L., Shirley, Y. L., & Loinard, L. 2005, ApJ, 632, 371
Chini, R. 1981, A&A, 99, 346
Claussen, M. J., Wilking, B. A., Benson, P. J., Wootten, A., Myers, P. C., & Terebey, S. 1996, ApJS, 106, 111
Elitzur, M. 1992, in Astronomical Masers (Dordrecht: Kluwer)
Hachisuka, K., et al. 2006, ApJ, 645, 337
Hirano, N., Mikami, H., Umemoto, T., Yamamoto, S., & Taniguchi, Y. 2001, ApJ, 547, 899
Hirota, T., et al. 2007, PASJ, 59, 897
Hirota, T., et al. 2008, PASJ, 60, in press
Honma, M., et al. 2007, PASJ, 59, 889
Honma, M., Kawaguchi, N., & Sasao, T. 2000, in Proc. SPIE, 4015, Radio Telescope, ed. H. R. Butcher, 624
Iguchi, S., Kurayama, T., Kawaguchi, N., & Kawakami, K. 2005, PASJ, 57, 259
Imai, H., Iwata, T., & Miyoshi, M. 1999, PASJ, 51, 473 (IIM99)
Imai, H., Kameya, O., Sasao, T., Miyoshi, M., Deguchi, S., Horiuchi, S., & Asaki, Y. 2000, ApJ, 538, 751
Imai, H., Sahai, R., & Morris, M. 2007, ApJ, 669, 424
Knude, J., & Høg, E. 1998, A&A, 338, 897
Kurayama, T., Sasao, T., & Kobayashi, H. 2005, ApJ, 627, L49
Matveyenko, L. I., Zhakharin, K. M., Diamond, P. J., & Gram, D. A. 2004, Astron. Lett., 30, 100
Moscadelli, L., Testi, L., Furuya, R. S., Goddi, C., Claussen, M., Kitamura, Y., & Wootten, A. 2006, A&A, 446, 985
Mundy, L. G., Wootten, A., Wilking, B. A., Blake, G. A., & Sargent, A. I. 1992, ApJ, 385, 306
Remijan, A. J., & Hollis, J. M. 2006, ApJ, 640, 842
Shimoikura, T., Kobayashi, H., Omodaka, T., Diamond, P. J., Matveyenko, L. I., & Fujisawa K. 2005, ApJ, 634, 459
Takakuwa, S., et al. 2007, ApJ, 662, 431
Wootten, A. 1993, in Astrophysical Masers, ed. A. W. Clegg & G. E. Nedoluha, (Heidelberg: Springer-Verlag), A11, C1, 315
Wootten, A., Claussen, M., Marvel, K., & Wilking, B. 1999, in the 3rd Cologne–Zermatt Symposium, ed. V. Ossenkopf, J. Stuzki, & G. Winnewisser (Herdecke: GCA-Verlag), 295